

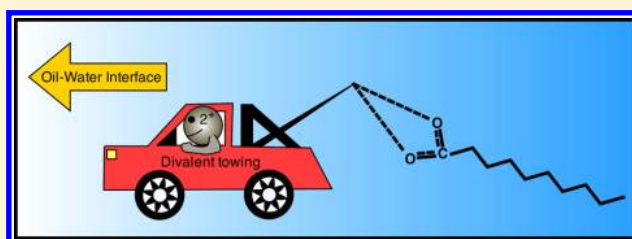
# Designated Drivers: The Differing Roles of Divalent Metal Ions in Surfactant Adsorption at the Oil–Water Interface

Ellen J. Robertson, Daniel K. Beaman, and Geraldine L. Richmond\*

Department of Chemistry, University of Oregon, Eugene, Oregon 97403, United States

## Supporting Information

**ABSTRACT:** Divalent metal ions play numerous roles in biological, technological, and environmental systems. This study examines the role of a variety of ions,  $\text{Mg}^{2+}$ ,  $\text{Ca}^{2+}$ ,  $\text{Mn}^{2+}$ ,  $\text{Ni}^{2+}$ ,  $\text{Cu}^{2+}$ , and  $\text{Zn}^{2+}$ , in the adsorption of sodium decanoate at the carbon tetrachloride–water interface. For all ions studied, the ions drive the adsorption of the surfactant to the interface. Using vibrational sum-frequency spectroscopy and the carboxylic acid vibrational modes as a signature for metal ion binding, each metal salt is found to play a distinctly different role in the molecular characteristics of surfactant adsorption at the interface. Additional spectroscopic studies of the methyl and methylene vibrations are monitored to track the ordering of the alkyl chains when metal salts are added to solution. How the metal–surfactant binding impacts the surfactant structure, orientation, and solvation is explored. How these spectroscopic measurements compare with the degree of adsorption as measured by interfacial tension data is presented.



## INTRODUCTION

The importance of metal binding is widespread throughout chemistry and biology. One of the most extensive chelators of metals are carboxylate groups which are present in familiar molecules such as EDTA as well as being the primary headgroup in fatty acids and soaps. Environmentally, humic acids have a particularly high carboxylic acid content and aid in the transport of both toxins (such as heavy metals) and nutrients through the soil. There have been extensive studies modeling humic acid to understand the binding activities of metal ions.<sup>1–9</sup> Metal ions also play an important role in a variety of biological processes.  $\text{Zn}^{2+}$  acts as a stabilizer for a collection of motifs known as zinc fingers, which contain 25–60 residues arranged around one or two  $\text{Zn}^{2+}$  ions and are important in the stabilization of small folded polypeptide chains that interact with nucleic acids.<sup>10</sup> In addition, metal ions, particularly transition metals, are required for catalysis in roughly one-third of all enzyme reactions. The transition metal ions, such as  $\text{Cu}^{2+}$  and  $\text{Mn}^{2+}$ , play a distinctly different role from monovalent ions like  $\text{Na}^+$  and  $\text{K}^+$ , which often act in a structural capacity rather than a catalytic one.<sup>10</sup> Also in contrast, monovalent ions tend to bind nonspecifically whereas divalent metal ions bind specifically to functional group such as phosphates, acting as superior shielding ions for large, highly structured biomolecules.<sup>10</sup> The presence of metals is also known to have a great effect on monolayers at the air–water interface, causing the monolayers to form a more condensed phase.<sup>11,12</sup> This has strong implications for intracellular structure near membrane walls, which are composed of fatty acids, phospholipids, and cholesterol.

Although bulk phase characteristics of metals binding to carboxylates have been extensively investigated, the importance

of these events at interfaces is only now becoming clear as environmental and biological studies provide more information about the existence of metals in interfacial chemistry. It is particularly important to understand the roles of metal ions in the behavior of carboxylates at the interface between two immiscible fluids, as these “soft” interfaces are ubiquitous in both biological and environmental systems. While there have been a number of studies at the air–water interface pertaining to metal binding with surface active species, these have primarily been conducted with spectroscopies that are not surface specific, and contributions from the bulk phase can have significant effects on the spectra.<sup>13–17</sup> Previous work by Allen and co-workers probed the carboxylate headgroup of long chain surfactants at the air–water interface with  $\text{Na}^+$ ,  $\text{K}^+$ ,  $\text{Ca}^{2+}$ , and  $\text{Mg}^{2+}$  and found distinct differences between the binding and deprotonating ability of these different ions.<sup>18–20</sup> Hühnerfuss and co-workers completed a number of studies on metals binding with carboxylates at the air–water interface using IR spectroscopy.<sup>13,14</sup> They categorized the types of binding based on the splitting between the symmetric and asymmetric stretching frequencies of the carboxylate headgroup. However, IR spectroscopy is not a surface specific technique, and analysis of the split between asymmetric and symmetric peaks is controversial, resulting in the strength of the binding interactions being undefined, especially since similar splitting parameters have been attributed to different metal ion–carboxylate interactions.<sup>13</sup>

Received: September 22, 2013

Revised: November 4, 2013

Published: November 22, 2013

In this work, vibrational sum-frequency (VSF) spectroscopy was used to study the interactions of group II and transition metal ions with carboxylate surfactants by probing the carboxylate headgroup and alkyl CH vibrational modes at the carbon tetrachloride–water ( $\text{CCl}_4\text{--H}_2\text{O}$ ) interface, a model for fluid interfaces found in biology and the environment. Based on the vibrational frequencies of the carboxylate symmetric stretch, it is possible to identify the coordination of several group II and transition metal ions with sodium decanoate adsorbed at the oil–water interface. Recent experiments in this lab have shown the oil–water interface to be a unique environment for surfactant headgroups, and the results proved the oil phase plays a large part in the distribution of orientations of the headgroup.<sup>21</sup> By using VSF spectroscopy in this study, the distribution of orientations of the headgroup is observed to change through vibrational frequency and peak amplitudes depending on the metal that is bound to it.

## ■ EXPERIMENTAL SECTION

**Spectroscopic Measurements.** VSF spectroscopic data were acquired with an Ekspla laser and IR generation system with a sample area built to accommodate the liquid–liquid cell and inverted beam geometries, where the visible and IR beams travel up through the  $\text{CCl}_4$  to the interface. This system has been described in detail elsewhere.<sup>22</sup> In short, a Nd:YAG laser outputs 1064 nm light with  $\sim 30$  ps pulse lengths. The 1064 nm light is split into two lines, and one line is frequency doubled to give 532 nm light. A small portion of the 532 nm line is used as the visible portion at the interface, while the remainder of the 532 nm line and the 1064 nm line are used to generate tunable infrared light via a typical OPG/OPA/DFG setup. In these experiments, all data were taken with the beams at their respective total internal reflection angles ( $23.5^\circ$  from the plane of the interface for the visible and  $15^\circ\text{--}17^\circ$  for the IR). Polarization changes of the IR beam were accomplished using periscopes on magnetic mounts.

The intensity of the detected sum-frequency signal as shown in eq 1 is proportional to the square of the effective second-order susceptibility  $\chi_{\text{eff}}^{(2)}$  and the intensity of the incident IR and visible beams.

$$I(\omega_{\text{sf}}) \propto |\chi_{\text{eff}}^{(2)}|^2 I(\omega_{\text{vis}}) I(\omega_{\text{IR}}) \quad (1)$$

The second-order susceptibility,  $\chi^{(2)}$ , as shown in eq 2 and the effective second-order susceptibility from eq 1 are related through the Fresnel coefficients and unit polarization vectors. Equation 2 shows that  $\chi^{(2)}$  is composed of a nonresonant component and the sum of all present resonant components.

$$\chi^{(2)} = \chi_{\text{NR}}^{(2)} + \sum_{\nu} \chi_{R_{\nu}}^{(2)} \quad (2)$$

The resonant second-order susceptibility,  $\chi_{R_{\nu}}^{(2)}$  as shown in eq 3, is dependent on both the number density of the molecules at the interface as well as the molecular hyperpolarizability,  $\beta$ . The angled brackets around  $\beta$  indicate that this is an average over all possible molecular orientations in the probed system.

$$\chi_{R_{\nu}}^{(2)} = \frac{N}{\epsilon_0} \langle \beta \rangle \quad (3)$$

The dependence of the sum frequency signal on the number density at the interface and the molecular orientation allows for a thorough perspective on interfacial adsorption. In addition, the polarization of the generated sum-frequency signal is dependent on the polarization of the visible and IR beams, and thus different polarization combinations can be used to probe different planes of the interface. In this study, polarization combinations ssp, sps, and ppp are used and the order of each polarization combination goes as the sum frequency, visible, and IR, respectively. ssp is used to probe components of the dipole that lie normal to the interfacial plane, sps is used to probe components of the

dipole that are in the plane of the interface, and ppp is sensitive to components that are both in and out of the plane of the interface.

The resulting spectra were fit using a convolution of a Gaussian and Lorentzian distribution described by Bain et al.,<sup>23</sup> shown in eq 4.

$$|\chi^{(2)}(\omega_{\text{SF}})|^2 = \left| \chi_{\text{NR}}^{(2)} + \sum_{\nu} \int_{-\infty}^{\infty} \frac{A_{\nu} e^{-[(\omega_{\text{L}} - \omega_{\nu})/\Gamma_{\nu}]^2}}{\omega_{\text{L}} - \omega_{\text{IR}} - i\Gamma_{\text{L}}} d\omega_{\text{L}} \right|^2 \quad (4)$$

This line shape takes into account both homogeneous broadening due to the inherent nature of the transition and inhomogeneous broadening due to the local environments of the molecules. For the fits, the Lorentzian line widths were held at constant values consistent with typical vibrational lifetimes,<sup>24–27</sup> while the Gaussian line widths were allowed to vary to account for the wide array of complex molecular environments, such as those due to hydrogen-bonding interactions.

The sample cell was designed from a solid piece of Kel-F and contains two windows set normal to the incident and outgoing 532 nm beam and are sealed with Dupont Kalrez perfluoropolymer O-rings. The input windows used were either  $\text{CaF}_2$  or  $\text{BaF}_2$ , and no difference was found in the spectra between the two. The output window was BK-7 glass as it only needed to transmit the generated visible sum-frequency light, and it was more robust toward the aggressive cleaning process used. All glassware, the cell, the BK-7 window, and the O-rings were soaked in concentrated sulfuric acid with No-Chromix for a minimum of 12 h, and then each piece was rinsed under water from an 18.2 M $\Omega$  Nanopure filtration system for at least 25 min. The  $\text{CaF}_2$  window was allowed to soak in the same acidic solution for 15–20 min and then copiously rinsed. The  $\text{BaF}_2$  window was used as is after gently wiping with lens tissue soaked with methanol.

Data acquisition started immediately after the interface was made and usually continued for approximately an hour for each prepared interface. Each spectrum shown in these experiments is an average of at least 300 laser shots per data point from at least three spectra that overlay each other within 5% error. In the cases where there was some equilibration time present in the initial spectra, then those spectra were not averaged into the data set. Long-term equilibration was checked by letting the interface sit for anywhere from 6 to 12 h and then retaking the spectra. In all cases there was no long-term time dependence observed in the spectroscopic data.

**Interfacial Tension Measurements.** Interfacial tension measurements were obtained using the Wilhelmy plate method with a balance purchased from KSV. The procedure for measuring the interfacial tension of the  $\text{CCl}_4\text{--H}_2\text{O}$  interface using the Wilhelmy plate method has been described previously.<sup>21</sup> This work showed that measurements made with the Wilhelmy plate method were within error of measurements obtained using the pendant drop method. For these studies, a similar procedure was used to obtain the interfacial tension of the metal–surfactant systems. A neat  $\text{CCl}_4\text{--H}_2\text{O}$  interface was first prepared in a dish, and a platinum plate attached to the balance was lowered to this interface to measure the interfacial tension. The cleanliness of the platinum plate and dish was confirmed if the interfacial tension was measured to be within 44–46 mN/m.<sup>28,29</sup> With the plate still sitting at the interface, an aliquot of concentrated sodium decanoate solution was added to the aqueous layer to obtain a bulk concentration of either 0.5 or 1 mM. This solution was measured until the interfacial tension value was observed to remain constant within  $\pm 0.2$  mN/m for 5 min. For the metal ion samples, aliquots of concentrated salt solutions were added to the aqueous sodium decanoate layer, and the interfacial tension was measured as discussed above.

**Sample Preparation.** Chemicals were purchased in the highest purity possible from Sigma-Aldrich (Na-dodecanoate, Na-decanoate, Metal Salts) and CDN Isotopes (d-K-dodecanoate 98.7% atom d). We could not obtain a deuterated dodecanoate with sodium as a counterion in a high enough purity for our spectroscopic measurements. Solutions were prepared using clean glassware, an analytical balance, and water from a Barnstead Nanopure system. Solution pH was tested using EMD pH paper with regular verification via an

Oakton 110 series pH meter. All salt–surfactant solutions were found to be in the range of pH 5–6. All metal salts in solution are specified as ionic strength in the presence of 1 mM Na-decanoate unless otherwise specified.

## RESULTS AND DISCUSSION

**Metal-Ion-Induced Surfactant Adsorption.** Group II metal ions such as  $\text{Ca}^{2+}$  and  $\text{Mg}^{2+}$  play important roles in biological systems where their binding to molecular species is essential for life functions.<sup>30</sup> Transition metals binding with organics are relevant to atmospheric chemistry as the presence of these ions can hinder reactions at the interface of cloud droplets.<sup>31</sup> Transition metals also play an important role biologically, as several are found in enzymatic systems.<sup>30</sup> We have therefore chosen to study the effects of a variety of metal ions ( $\text{Mg}^{2+}$ ,  $\text{Ca}^{2+}$ ,  $\text{Mn}^{2+}$ ,  $\text{Ni}^{2+}$ ,  $\text{Cu}^{2+}$ , and  $\text{Zn}^{2+}$ ) on the assembly behavior of sodium decanoate at an aqueous/hydrophobic interface in order to determine the specific effects of each ion and how these effects relate to overall macromolecular interfacial behavior. First, in order to determine the degree to which these metal ions affect the relative amount of sodium decanoate adsorbed to the  $\text{CCl}_4$ – $\text{H}_2\text{O}$  interface, interfacial data were obtained for sodium decanoate both with and without metal ions. These data are shown in Figure 1.

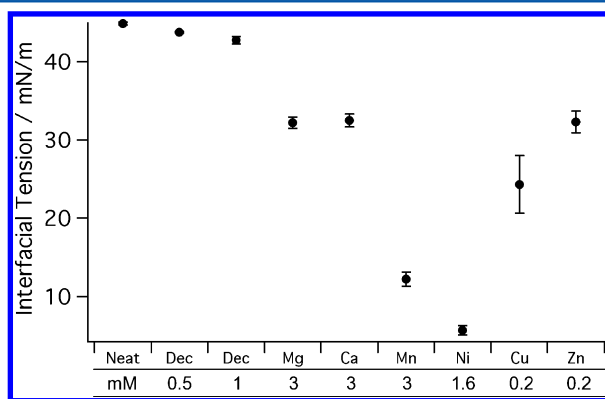


**Figure 1.** Interfacial tension measurements for the six ions at the  $\text{CCl}_4$ – $\text{H}_2\text{O}$  interface as well as the interfacial tension of the two concentrations of sodium decanoate and the neat interface. Concentrations are those used in the VSF spectroscopy experiments.

From the plot, it is shown that the metal-free sodium decanoate solutions only somewhat reduce the interfacial tension of the neat  $\text{CCl}_4$ – $\text{H}_2\text{O}$  interface from  $\sim 45$  to  $\sim 42$  mN/m for the 1 mM sample. Additionally, we observed that the aqueous metal ion solutions in the absence of surfactant did not significantly reduce the interfacial tension below 44 mN/m. It is clear, however, that each of the ions studied increases the degree of adsorption of sodium decanoate at the oil–water interface, albeit to different degrees. At a metal ion concentration of 3 mM,  $\text{Mg}^{2+}$  and  $\text{Ca}^{2+}$  have similar effects, reducing the interfacial tension to  $\sim 30$  mN/m, while  $\text{Mn}^{2+}$  reduces the interfacial further to  $\sim 12$  mN/m. Even at a lower metal ion concentration of 1.6 mM,  $\text{Ni}^{2+}$  is able to reduce the interfacial tension more than the other ions to  $\sim 7$  mN/m. Because of solubility constraints,  $\text{Cu}^{2+}$  and  $\text{Zn}^{2+}$  were studied at a concentration of only 200  $\mu\text{M}$ , yet with sodium decanoate they are still able to reduce the interfacial tension values to  $\sim 20$  and 30 mN/m, respectively.

From this data, it is obvious that each metal ion plays a specific role in driving sodium decanoate to the oil–water interface. In order to understand the molecular level factors that contribute to the metal-ion-induced adsorption of sodium decanoate to the oil–water interface, interactions between the specific metal ion and the carboxylate headgroup must be characterized at the interface. This will be accomplished through VSF spectroscopic studies of the carboxylate stretching region. An analysis is first required of the behavior of metal-ion-free carboxylates at the oil–water interface so that spectral features associated with metal ion–carboxylate interactions can be characterized.

**Carboxylates at the Oil–Water Interface.** Previous work in this lab has shown that carboxylate surfactants adopt a wide distribution of orientations at the oil–water interface due to the large area per headgroup, the solvation of the chains via the oil phase, and the variety of possible hydrogen bonding of water to the headgroup of the surface adsorbed surfactant.<sup>21</sup> Figure 2 shows VSF spectra in the carboxylate stretching region for sodium dodecanoate.

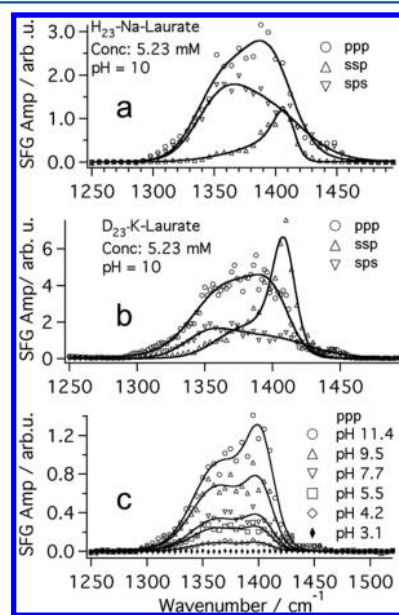


**Figure 2.** VSF spectra of (a)  $\text{H}_{23}$ –Na-dodecanoate in spp, spp, and ppp polarization schemes, (b)  $\text{D}_{23}$ –K-dodecanoate in the spp, spp, and ppp polarizations schemes, and (c) pH series of  $\text{H}_{23}$ –Na-dodecanoate in the ppp polarization scheme.

Figure 2a shows VSF spectra in spp, spp, and spp polarization schemes of the carboxylate headgroup symmetric stretch. The same spectra for the three polarization schemes of a fully deuterated sample (Figure 2b) removes any overtone or combination band contributions. Although differences in the carboxylate spectra with  $\text{Na}^+$  compared to  $\text{K}^+$  may be due to differences in counterion interactions with the headgroup, the deuterated spectra in Figure 2b clearly confirm that the primary spectral features in Figure 2a are due to carboxylate headgroup vibrations. Further proof of this was found in a pH series of Na-dodecanoate in spp polarization (Figure 2c) where the full width of the modes is observed to decrease as the pH is lowered. As the headgroup is protonated to become a carboxylic acid, all the vibrational modes in the carboxylate region disappear. The spectra of the carboxylate region can be fit to two vibrational modes in this region: one centered at approximately  $1370 \text{ cm}^{-1}$

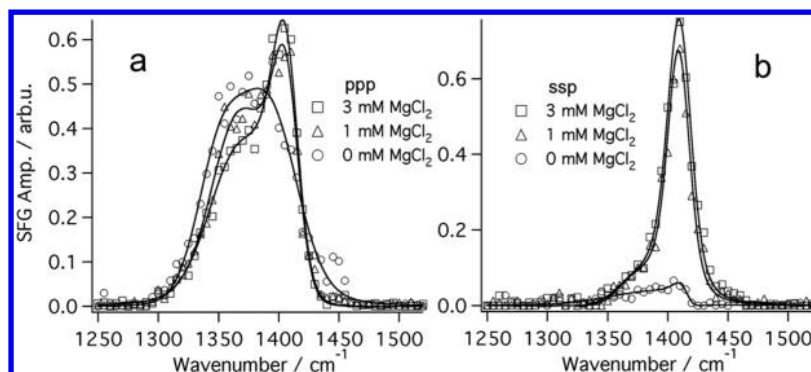


**Figure 3.** The ppp (a) and ssp (b) VSF spectra of 1 mM sodium decanoate at pH 5.5 with  $\text{MgCl}_2$  in the  $\text{COO}^-$  region. The solid lines are fits to the data.

and the other at  $1405\text{ cm}^{-1}$ .<sup>32</sup> The two modes correspond to different hydrogen-bonding structures of the headgroup at the interface. Although only two peaks can be resolved spectroscopically, the breadth of these peaks implies that there is an extent of possible hydrogen bonding environments. In this continuum of environments, the lower frequency peak is due to a more hydrogen bound headgroup, and the higher frequency peak is due to a less hydrogen bound headgroup. This is similar to the interpretations of VSF water spectra where the hydrogen-bonding coordination number leads to shifts of  $700\text{ cm}^{-1}$  or more.<sup>33–35</sup> The broad widths of the spectra and the distinguishable hydrogen-bonded frequencies of the headgroups makes this an excellent case study for the binding of ions to the charged surfactants because any change in the headgroup hydrogen-bonding structure, such as through the ionic or covalent binding of metal ions, will be apparent in the VSF spectral signatures.

**Ionic Metal Ion–Carboxylate Interactions.** VSF spectra were taken in the carboxylate region for the sodium decanoate–metal ion systems in order to determine the effects of each specific metal ion on the surfactant headgroup and how this relates to induced surfactant adsorption at the oil–water interface. Overall, the spectra for sodium decanoate with  $\text{Mg}^{2+}$ ,  $\text{Ca}^{2+}$ ,  $\text{Mn}^{2+}$ , and  $\text{Ni}^{2+}$  look very similar. The VSF spectra in the carboxylate region for sodium decanoate with  $\text{Mg}^{2+}$  are shown in Figure 3 as a representation of the spectral changes observed with these ions compared to the neat sodium decanoate spectra.

Clear changes are observed in the ppp polarization (Figure 3a) and ssp polarization (Figure 3b) spectra that indicate metal ion interactions with the carboxylate groups. First, the ppp spectra show a blue-shift in both the peak near  $1345\text{ cm}^{-1}$  to  $1357\text{ cm}^{-1}$  and the peak near  $1400\text{ cm}^{-1}$  to  $1414\text{ cm}^{-1}$ . This indicates that the presence of an ion–headgroup interaction is disrupting the hydrogen-bonding network present for the carboxylate group of sodium decanoate in the absence of metal ions by displacing water molecules near the surface of the headgroup to form the carboxylate salt.

Additionally, both the ppp and ssp spectra show a decrease in the amplitude of the peak near  $1345\text{ cm}^{-1}$  while concurrently showing an increase in the amplitude of the peak near  $1400\text{ cm}^{-1}$ . As discussed above, the lower frequency peak, which has a large amplitude in the ssp polarization scheme, is assigned to carboxylate groups in a more strongly hydrogen bonded environment that mostly exist in an orientation in the plane of the interface. On the other hand, the high-frequency peak, which has a large amplitude in the ppp polarization scheme, is

assigned to carboxylate groups in a less strongly hydrogen bonded environment that mostly exist in an orientation normal to the plane of the interface. The decrease in amplitude of the low-frequency peak along with the increase in amplitude of the high-frequency peak therefore suggests that the metal ion–carboxylate interactions cause a net change in the orientation of groups that are in the plane of the interface to being more upright at the interface. This is confirmed by the ssp spectrum of sodium decanoate in the presence of  $\text{Mg}^{2+}$ , which shows a decrease in intensity in the carboxylate region compared to the metal-free spectrum. For clarity of the figure, this data is not shown.

Although the decrease in interfacial tension for the  $\text{Mg}^{2+}$ –decanoate system suggests that a change in the headgroup to a more upright orientation is due to an increase in the number of surfactant molecules at the interface and thus an increase in packing, our previous VSF spectroscopic and interfacial tension studies of lauric acid as a function of concentration imply that this is not the case. These studies show that an increase in the bulk concentration results in both a decrease in interfacial tension and an increase in the peak amplitudes for both the peak near  $1370$  and  $1405\text{ cm}^{-1}$ .<sup>21</sup> Thus, an increase in bulk surfactant concentration mainly results in an increase in the number of surfactant molecules at the interface, with no significant changes in the overall orientation of the surfactant headgroup.

With  $\text{Mg}^{2+}$ , however, a decrease in interfacial tension is accompanied by a change in headgroup orientation, indicating that the metal ion–carboxylate interactions are responsible for this phenomenon. We attribute the headgroup reorientation to two factors. First, metal ion–carboxylate interactions decrease the degree of water solvation of the headgroups, which in the previous concentration study was found to be the dominant factor in headgroup orientation. Second, ionic interactions between the metal ion and carboxylate groups screen the charges of the headgroup, such that unfavorable charge–charge repulsion between neighboring adsorbed surfactants is reduced so that carboxylate groups can more easily align at the interface. Such ionic interactions are known to occur for the metal ions discussed in this section.<sup>36</sup>

By looking at the degree of these spectral changes compared to the metal ion-free sodium decanoate spectra, we can determine the relative extent of the metal–carboxylate ionic interactions for different metal ions. For example, similar spectral changes seen with  $\text{Mg}^{2+}$  are also observed with  $\text{Ca}^{2+}$  (Figure S1) and  $\text{Mn}^{2+}$  (Figure S2), yet the degrees of these changes are different. Briefly,  $\text{Ca}^{2+}$  induces a slightly larger

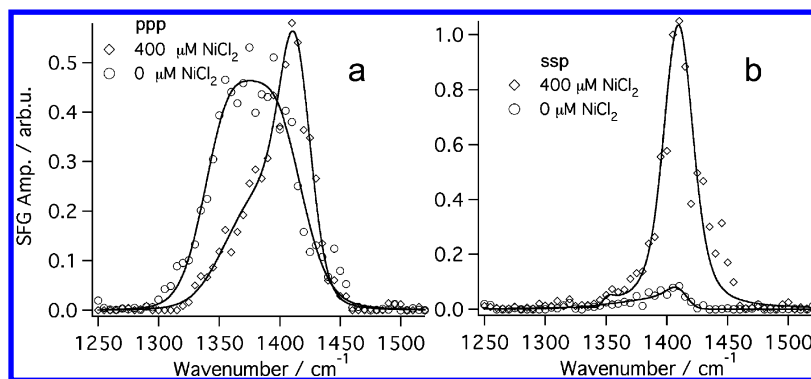


**Figure 4.** The ppp (a) and ssp (b) VSF spectra of 1 mM sodium decanoate at pH 5.5 with  $\text{NiCl}_2$  in the  $\text{COO}^-$  region. The solid lines are fits to the data.

increase in amplitude of the peak near  $1400\text{ cm}^{-1}$  compared to  $\text{Mg}^{2+}$ , showing that  $\text{Ca}^{2+}$  has a somewhat stronger ionic interaction with the carboxylate groups than  $\text{Mg}^{2+}$ . Furthermore,  $\text{Mn}^{2+}$  shows a greater blue-shifting of the higher frequency carboxylate peak compared to either  $\text{Mg}^{2+}$  or  $\text{Ca}^{2+}$ , indicating that  $\text{Mn}^{2+}$  interacts more strongly with the carboxylate groups than either  $\text{Mg}^{2+}$  or  $\text{Ca}^{2+}$ . Information on peak positions and amplitudes for each metal ion are presented in Tables S1 and S2, respectively.

While the VSF spectra in the carboxylate region for sodium decanoate with  $\text{Ni}^{2+}$  again look similar to the spectra of the other metal ions discussed above, the spectral changes compared to sodium decanoate in the absence of metal ions are much more pronounced. Figure 4 contains the VSF spectra of  $\text{NiCl}_2$  at an ionic strength of  $400\text{ }\mu\text{M}$  in the presence of 1 mM sodium decanoate.

As seen in the ppp spectra (Figure 4a), the lower frequency component decreases in amplitude significantly while the higher frequency component not only increases in amplitude but also blue-shifts significantly from  $1400$  to  $1420\text{ cm}^{-1}$ . In the ssp spectra (Figure 4b), although the  $\text{Ni}^{2+}$  is at an ionic strength 6 times less than that of the  $\text{Mg}^{2+}$  shown in Figure 3, it shows an even greater amplitude decrease of the low-frequency carboxylate peak and amplitude increase of the high-frequency carboxylate peak over the neat 1 mM Na-decanoate ssp spectra compared to the 3 mM  $\text{Mg}^{2+}$  solution. The induced shift and the amplitude changes both indicate that  $\text{Ni}^{2+}$  is by far the strongest bound ion introduced thus far. While  $\text{Mg}^{2+}$ ,  $\text{Ca}^{2+}$ , and  $\text{Mn}^{2+}$  are known to bind with ionic character,<sup>36</sup>  $\text{Ni}^{2+}$  is thought to bind with character between that of ionic and monodentate.<sup>13,37</sup> These results provide evidence that the binding strength of the  $\text{Ni}^{2+}$  with a carboxylate is much stronger than that of the other three ions. However, if the binding were hydrogen-bonded monodentate in character, the spectra would be expected to shift much more significantly than what is observed here, with the peak appearing at a frequency greater than  $1430\text{ cm}^{-1}$ .

It is clear that the strength of the ionic interaction between the metal ions and the carboxylate groups plays a strong role in increased adsorption of sodium decanoate to the oil–water interface, as seen in the interfacial tension data shown in Figure 1. Here, the trend in the degree of increased adsorption follows the trend for ionic interaction strength:  $\text{Mg}^{2+} \approx \text{Ca}^{2+} < \text{Mn}^{2+} < \text{Ni}^{2+}$ . We attribute this to the degree to which the specific metal ion interacts with the carboxylate headgroup. The better the metal ion is both able to displace water from and screen the charge of the carboxylate headgroup, the better the surfactants

are able to assemble at the interface due to decreased water solubility and reduced charge–charge repulsions.

**Covalent Metal Ion–Carboxylate Interactions.** While the above metal ion studies clearly demonstrated the role of ionic interactions in induced surfactant adsorption to the oil–water interface, they were unable to show how the much stronger covalent bonding interactions between carboxylate groups and metal ions dictate surfactant interfacial behavior. In order to distinguish between ionic and covalent binding character, two ions were investigated that are known to have stronger covalent binding characteristics with carboxylates,  $\text{Cu}^{2+}$  and  $\text{Zn}^{2+}$ .<sup>36</sup> Because of solubility constraints, these ions were studied at much lower concentrations than the ions above; however, the effects of these ions on the VSF spectra of sodium decanoate even at low concentrations leave no doubt as to the ability to distinguish between ionic binding character and covalent binding character. Spectra of 0.5 mM sodium decanoate with and without  $\text{Cu}^{2+}$  in the ssp polarization scheme are shown in Figure 5.

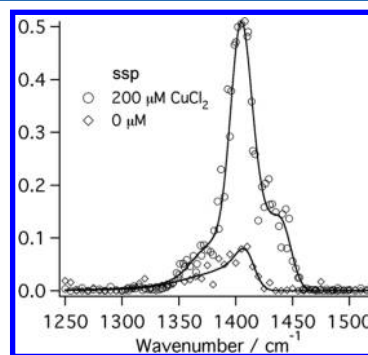


**Figure 5.** The ssp VSF spectra of  $\text{CuCl}_2$  ( $I = 200\text{ }\mu\text{M}$ ) and sodium decanoate (0.5 mM) in the  $\text{COO}^-$  region. The solid lines are fits to the data.

In ppp (Figure S3), the spectral shape is similar to the other ions between  $1300$  and  $1400\text{ cm}^{-1}$ , indicating that some of the  $\text{Cu}^{2+}$  ions may be interacting with the carboxylate groups in an ionic fashion. However, with  $\text{Cu}^{2+}$ , a third mode appears at  $1450\text{ cm}^{-1}$  that is seen in both the ppp and ssp spectra. This mode is also assigned to the carboxylate symmetric stretch. Carboxylates bound to metal ions in a bidentate fashion are known to produce distinct vibrations within the carboxylate stretching region.<sup>38–40</sup> The mode at  $1450\text{ cm}^{-1}$  is attributed to the bound carboxylate headgroups where a  $\text{Cu}^{2+}$  ion is interacting with it in a bidentate manner.<sup>36</sup>

Because of the largely different results between  $\text{Cu}^{2+}$  and the other ions, a study of  $\text{Zn}^{2+}$  was necessary to further characterize the specific type of binding between ions and the headgroup. The VSF spectrum of sodium decanoate with  $\text{Zn}^{2+}$  in the ssp polarization scheme of the carboxylate region is shown in Figure 6.

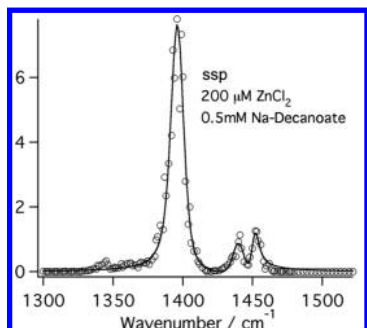


**Figure 6.** The ssp polarization VSF spectrum of the  $\text{COO}^-$  vibrational region for  $\text{ZnCl}_2$  ( $I = 200 \mu\text{M}$ ) and sodium decanoate (0.5 mM). The solid lines are fits to the data.

The ppp spectrum with  $\text{Zn}^{2+}$  (Figure S4) again shows the same modes between  $1300$  and  $1400 \text{ cm}^{-1}$  observed in the spectra for the metals that interact with the carboxylate groups in a purely ionic manner. In the ssp spectra of  $\text{Zn}^{2+}$ , there is a strong mode at  $1395 \text{ cm}^{-1}$  and two weaker modes at  $1435$  and  $1450 \text{ cm}^{-1}$  that are not observed in the spectra of metal ions that interact with the carboxylate groups in a purely ionic manner. Once again, these modes are all assigned to carboxylate symmetric stretches. As with the  $\text{Cu}^{2+}$  spectra, significant splitting is observed. Here, this splitting is in part attributed to different  $\text{Zn}^{2+}$ -carboxylate interactions,<sup>38</sup> with the peak near  $1435 \text{ cm}^{-1}$  characteristic of either a hydrogen-bonded monodentate or bridging complex, and the peak near  $1450 \text{ cm}^{-1}$  characteristic of a bidentate complex.<sup>19,36</sup> These  $\text{Zn}^{2+}$ -carboxylate complexes are consistent with what has been suggested for  $\text{Zn}^{2+}$  bound octadecanoic acid monolayers at the air-water interface.<sup>13</sup>

It is clear from the interfacial tension and VSF spectroscopic studies of sodium decanoate with  $\text{Cu}^{2+}$  and  $\text{Zn}^{2+}$  that like ionic interactions, covalent binding interactions between metal ions and the carboxylate headgroups act to drive surfactant molecules to the interface, even at metal ion concentrations as low as  $200 \mu\text{M}$ . A stronger effect than the role of ionic interactions in induced surfactant adsorption, covalent metal

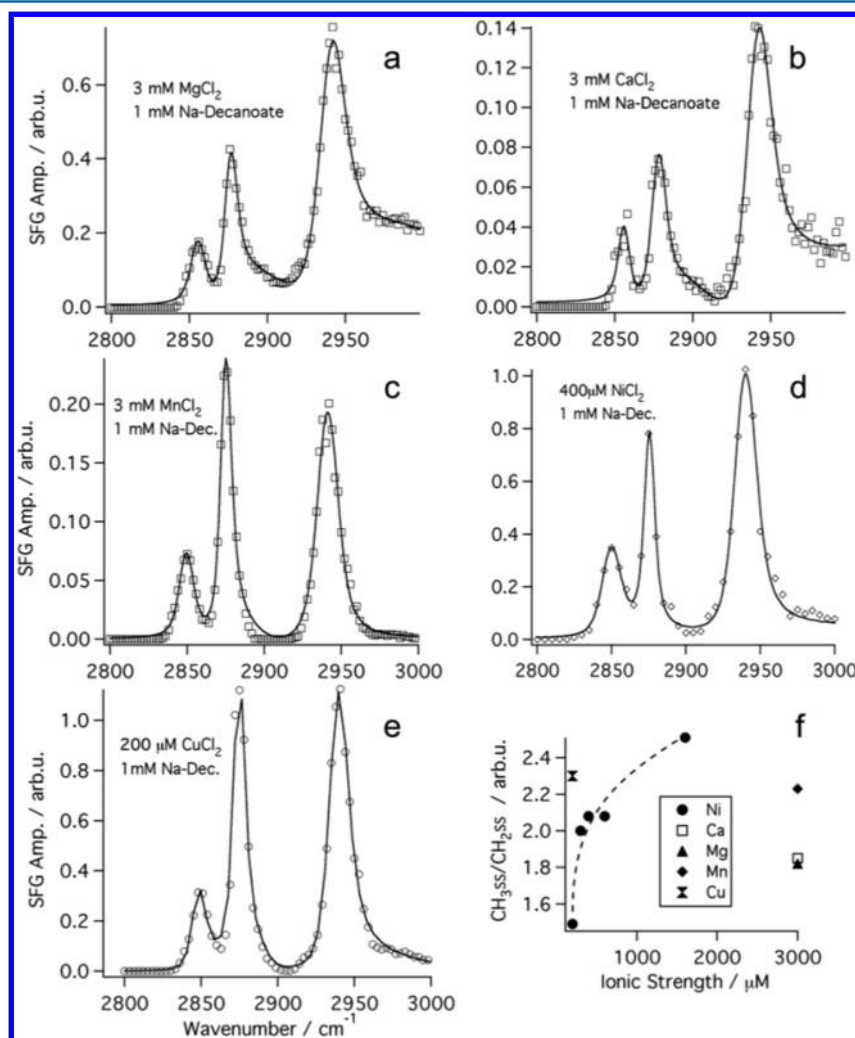


**Figure 7.** The ssp polarization VSF spectra of the CH vibrational region for sodium decanoate with the metal ions studied. The solid lines are fits to the data.

binding to the carboxylate groups would completely displace water from and screen the charge of the headgroups, driving the surfactant to the oil–water interface. Even though from the interfacial tension data it appears that  $\text{Zn}^{2+}$  does not induce the adsorption of sodium decanoate to the interface to the same extent as  $\text{Cu}^{2+}$ , the larger amplitudes of the carboxylate peaks seen for  $\text{Zn}^{2+}$  compared to  $\text{Cu}^{2+}$  indicate that  $\text{Zn}^{2+}$  induces a stronger orientation of the carboxylate groups at the interface. We attribute this to the different types of covalent interactions that occur between  $\text{Zn}^{2+}$  and the carboxylate groups.

While the above analysis of the VSF spectra of the carboxylate region for sodium decanoate with metal ions was able to show the effect of specific metal ion–headgroup interactions on induced surfactant adsorption and carboxylate orientation at the oil–water interface, this information does not provide a relationship between the degree of induced adsorption and the degree of alkyl chain orientation. The reduction in interfacial tension for sodium decanoate with the metal ions compared to the metal free solutions suggests an increase in favorable alkyl chain interactions between neighboring interfacial surfactants due to tight packing of the molecules at the interface. VSF spectra of the CH stretching region, however, are required for determining the specific molecular level degree of surfactant chain orientation and how the metal ion interactions with the carboxylate headgroups affects this orientation.

**Alkyl Chain Conformations.** VSF spectra in the CH stretching region in the ssp polarization scheme are shown in Figure 7 for the ions studied. The spectra are fit to four vibrational modes. From low to high frequency, they appear near 2850, 2880, 2910, and 2940  $\text{cm}^{-1}$ . Additional peaks did not improve the quality of the fits. These are assigned to the methylene symmetric stretch ( $\nu_s\text{CH}_2$ ), the methyl symmetric stretch ( $\nu_s\text{CH}_3$ ), the methylene Fermi resonance ( $\nu_{\text{fr}}\text{CH}_2$ ), and the methyl Fermi resonance ( $\nu_{\text{fr}}\text{CH}_3$ ), respectively. Fitting the amplitudes of the peaks allows a direct assessment of the chain conformation, given that methylene vibrations are only observed with VSF spectroscopy when the cylindrical symmetry of the chain is broken via a gauche defect. In instances where methylene vibrations are observed, an order parameter may be calculated as the ratio of methyl/methylene amplitude as an internal method of comparing the ordering of the interfacial surfactant chains within a set of experiments.<sup>41–43</sup>

The ratios of the methyl/methylene vibrations are shown in Figure 7f for each of the ions studied in this work.  $\text{Mg}^{2+}$  (Figure 7a) and  $\text{Ca}^{2+}$  (Figure 7b) show the lowest ratio, indicating that these two ions induce the lowest amount of monolayer ordering even though they are at the highest ionic strength used in this work.  $\text{Mn}^{2+}$  (Figure 7c) induces a significantly larger amount of ordering within the monolayer, followed by  $\text{Ni}^{2+}$  (Figure 7d). In Figure 7f,  $\text{Ni}^{2+}$  is shown as a concentration series, and more details will be discussed in the following section. At half the ionic strength of  $\text{Mn}^{2+}$ ,  $\text{Ca}^{2+}$ , and  $\text{Mg}^{2+}$ ,  $\text{Ni}^{2+}$  induces more chain ordering. For these metals which have been shown to interact with the carboxylate groups at the interface in a purely ionic manner, the degree of alkyl chain ordering follows the trend of the degree of the metal ion interaction with the surfactant headgroup as well as the degree of induced surfactant adsorption. This confirms that the strength of the ionic interaction between the metal ion and the carboxylate group drives the surfactant to the interface in a more tightly packed monolayer where both the headgroup and alkyl chains are highly ordered.

At only 200  $\mu\text{M}$ ,  $\text{Cu}^{2+}$  (Figure 7e) shows by far the largest enhancement in alkyl ordering for a given concentration. Although  $\text{Ni}^{2+}$  does have a larger order parameter at 1.6 mM, this is a factor of 8 greater in ionic strength and is thus not surprising. It is interesting, however, that even though  $\text{Cu}^{2+}$  seems to induce the greatest degree of order compared to the metal ions studied, it does not reduce the interfacial tension of sodium decanoate as significantly as either  $\text{Mn}^{2+}$  or  $\text{Ni}^{2+}$ . Because fewer surfactant molecules adsorb to the interface with  $\text{Cu}^{2+}$  due to smaller surfactant and metal ion concentrations, this higher degree of alkyl chain orientation is unexpected. It has been suggested, however, that covalent bidentate interactions between metal ions and adsorbed surfactant headgroups can induce alkyl chains to adopt an *all-trans* configuration to maximize favorable chain–chain interactions at the interface.<sup>19</sup> Previous studies have observed this same effect at the air–water interface for fatty acids, where the bidentate binding of metal ions to carboxylate containing surfactants causes the condensation of monolayer alkyl chains.<sup>13,15,16,37</sup> This induces an increase in molecular packing and orientation of molecules at the air–water interface.

For  $\text{Zn}^{2+}$ , an order parameter of  $\sim 1$  was obtained, which is lower than for any other metal ion studied. For clarity of the figure, this data is not shown. We attribute this lower ordering of the surfactant chains in the presence of  $\text{Zn}^{2+}$  to the very different binding behavior of this metal ion with the carboxylate headgroup compared to the other metal ions. Because of these multiple covalent binding interactions, it is likely that other effects are at play in chain ordering, such as the coordination of multiple carboxylate groups to one ion.<sup>38</sup>

**A Closer Inspection of  $\text{NiCl}_2$ .** Of the six ions in this study,  $\text{Ni}^{2+}$  is unique as its binding characteristics are typically defined as being between what is categorized as ionic or covalent.<sup>13,37</sup> This is attributed to a relatively weak covalent interaction that is thought to be monodentate in nature, making it difficult to distinguish a purely covalent interaction from a purely ionic interaction. The unique ability to look at the binding interactions directly at the interface in this study makes it possible to better characterize this interaction and definitively state whether  $\text{Ni}^{2+}$  is interacting in a covalent or ionic fashion. As discussed above,  $\text{Zn}^{2+}$  and  $\text{Cu}^{2+}$  gave distinct spectral signatures that indicated they were binding in a covalent manner. In order to understand the binding nature of  $\text{Ni}^{2+}$ , a full concentration series was completed to observe the shifting of the vibrational modes.

Figure 8 shows VSF spectra of 1 mM sodium decanoate with  $\text{NiCl}_2$  at concentrations from 50  $\mu\text{M}$  to 1.6 mM in the ssp polarization scheme. The ppp spectra (Figure S5) show a blue-shifting trend in the peaks as salt concentration is increased, and the low-frequency component decreases significantly in amplitude as it blue-shifts. In ssp polarization the carboxylate mode grows in amplitude, and a shoulder appears on the high-frequency side as concentration is increased. This peak near 1450  $\text{cm}^{-1}$  appears in the spectra for  $\text{Cu}^{2+}$  (Figure 5) and  $\text{Zn}^{2+}$  (Figure 6) and is attributed to the metals binding to the carboxylate groups in a bidentate manner. The appearance of the 1450  $\text{cm}^{-1}$  peak in the ssp spectrum of  $\text{Ni}^{2+}$  at 1.6 mM is evidence that at higher ion concentrations  $\text{Ni}^{2+}$  also binds to the carboxylate groups in a bidentate manner.

To further investigate the effects of  $\text{Ni}^{2+}$  on the interfacial sodium decanoate molecules, the water and CH region were monitored as a function of  $\text{Ni}^{2+}$  concentration. As shown in Figure 9, the concentration of  $\text{Ni}^{2+}$  has a large effect on the

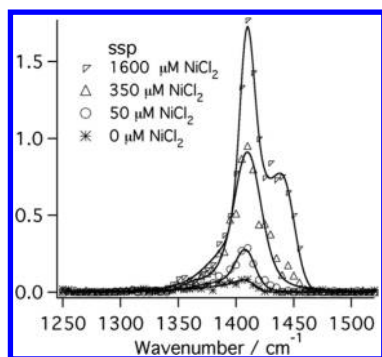


**Figure 8.** The ssp polarization VSF spectra of the  $\text{COO}^-$  region for the  $\text{NiCl}_2$  concentration series with 1 mM sodium decanoate. The solid lines are fits to the data. Some concentrations are omitted for clarity.

alkyl chain ordering. In addition, it was also shown that  $\text{Ni}^{2+}$  caused the largest drop in interfacial tension of 1 mM sodium decanoate.

Figure 9a presents water and alkyl region VSF spectra for a  $\text{Ni}^{2+}$  concentration series. At 50  $\mu\text{M}$  concentration, the water spectrum looks like that of a typical charged surfactant at the interface. There are CH modes between 2800 and 3000  $\text{cm}^{-1}$  and a broad water peak centered at 3200  $\text{cm}^{-1}$ , which is typically assigned to a highly coordinated water species at the interface. As the ionic strength of  $\text{Ni}^{2+}$  is increased, two regions of the spectra show significant change. The CH modes grow in amplitude and become more distinct as shown in Figure 9b. The  $\text{Ni}^{2+}$  concentration series is fit in the CH region, and the methyl to methylene ratio is analyzed and plotted in Figure 7f. It is concluded that as  $\text{Ni}^{2+}$  concentration is increased, the ordering of the alkyl chains increases. At 200  $\mu\text{M}$ , the conformation of the alkyl chains is disordered; however, the conformation rapidly increases, and by 300  $\mu\text{M}$ , the ordering within the monolayer has already surpassed that of  $\text{Ca}^{2+}$  and  $\text{Mg}^{2+}$  at 3 mM ionic strength. The broad water mode centered at 3200  $\text{cm}^{-1}$  decreases to zero intensity. The electric field at the interface from the adsorbed surfactants that is due to the double layer acts to orient these strongly coordinated water molecules, and thus they contribute strongly to the VSF spectra when the field is not neutralized. However, as more  $\text{Ni}^{2+}$  is added to solution, the field at the interface becomes negligible as the charges on the surfactants become neutralized, and hence orientation of the water molecules within the interfacial region disappears. In addition, the ions displace the water solvating the headgroup, and thus the number density of water molecules

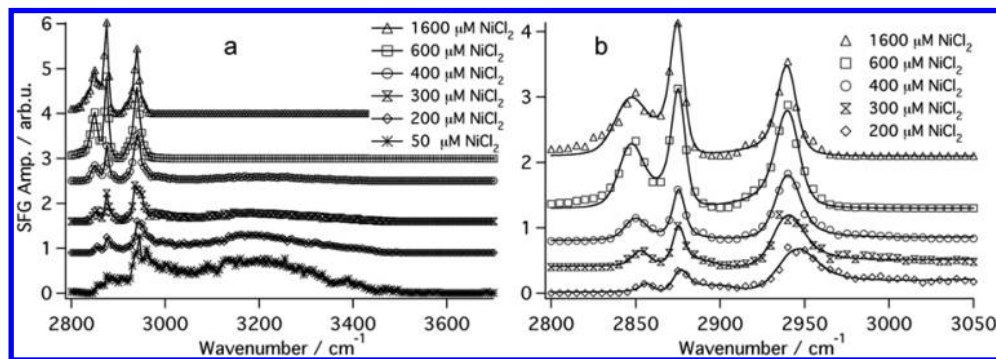


**Figure 9.** VSF spectra of the water and CH vibrational region for the  $\text{NiCl}_2$  concentration range investigated. The solid lines are fits to the data, which can be used to extract alkyl conformational changes over the concentration range. Spectra are offset for clarity.

within the interfacial region is also decreasing. The combination of these two effects leads to the loss of water signal in the spectra. The neutralization of the interface is observed at a  $\text{Ni}^{2+}$  ionic strength around 400  $\mu\text{M}$ . Relative to bulk concentrations, this means there is only one nickel ion present for every 7–8 surfactant molecules. However, at the interface, an excess of  $\text{Ni}^{2+}$  ions is likely to exist due to the inherent interfacial field,<sup>22</sup> and thus neutralization of the monolayer occurs at very low bulk concentrations of the ion.

## SUMMARY AND CONCLUSIONS

Our VSF spectroscopic and interfacial tension studies have shown that metal ions induce the adsorption of sodium decanoate to the  $\text{CCl}_4\text{-H}_2\text{O}$  interface through both ion and covalent interactions of the metal ion with the carboxylate headgroup. Figure 10 summarizes the specific interactions for the ions studied.

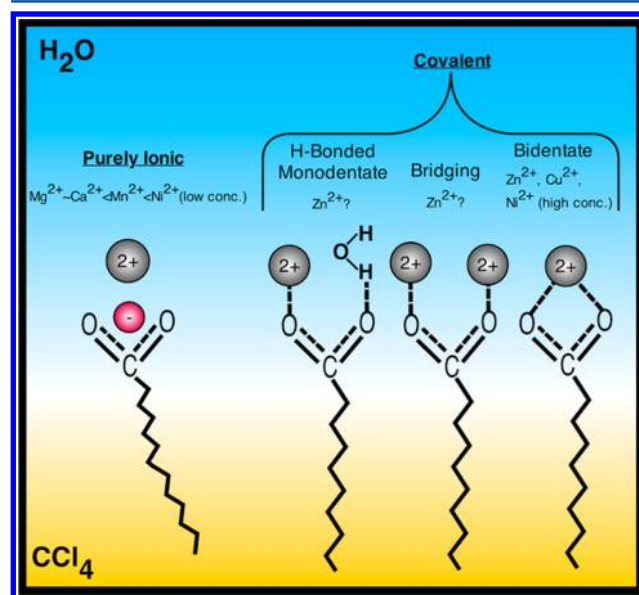


**Figure 10.** Cartoon depicting the metal ion–carboxylate group interactions observed at the  $\text{CCl}_4\text{-H}_2\text{O}$  for the different metal ions studied with sodium decanoate.

$\text{Mg}^{2+}$ ,  $\text{Ca}^{2+}$ ,  $\text{Mn}^{2+}$ , and  $\text{Ni}^{2+}$  (at low  $\text{Ni}^{2+}$  concentration) were found to interact with the headgroup of the surfactant in a purely ionic manner, and the strength of this interaction ( $\text{Mg}^{2+} \approx \text{Ca}^{2+} < \text{Mn}^{2+} < \text{Ni}^{2+}$ ) determined the degree to which the



surfactant adsorbed to the interface as a tightly packed, more highly ordered monolayer.  $\text{Zn}^{2+}$  and  $\text{Cu}^{2+}$  were found to interact with the carboxylate headgroups in a covalent manner. This stronger interaction, compared to purely ionic interactions, allowed  $\text{Zn}^{2+}$  and  $\text{Cu}^{2+}$  to induce the adsorption and orientation of sodium decanoate at the  $\text{CCl}_4\text{-H}_2\text{O}$  interface at a far lower metal ion concentration than was seen for the other metal ions. Different specific covalent interactions with the carboxylate groups were found to occur for  $\text{Cu}^{2+}$  (bidentate) and  $\text{Zn}^{2+}$  (bidentate and either bridging or hydrogen-bonded monodentate). While  $\text{Cu}^{2+}$  was found to induce the adsorption of sodium decanoate to the interface to a greater degree than  $\text{Zn}^{2+}$ , the different covalent interaction of  $\text{Zn}^{2+}$  with the carboxylate groups were found to induce a greater degree of headgroup orientation.  $\text{Ni}^{2+}$  showed unique behavior, in that it was found to bind in a purely ionic manner at low concentration, with evidence for covalent bidentate interactions at higher  $\text{Ni}^{2+}$  concentrations. The mechanism for metal-ion-induced surfactant adsorption and ordering at the oil–water interface was determined to be the exclusion of water from and the charge screening of the surfactant headgroup due to the metal ion–carboxylate interactions. These factors act to both reduce the water solubility of the surfactant and minimize charge–charge repulsions at the interface.

That different ions are able to enhance the degree of monolayer packing and ordering at an oil–water interface depending on binding strength has implications for both environmental and biological systems. Environmentally, humic substances are carboxylate-containing surfactants that are known to bind toxic metals, and the fate and transport of such toxins is a topic of concern. Our results show that metal ions that are better able to bind carboxylate groups are better able to accumulate at oil–water interfaces, suggesting that such strong metal binders to humic substances can accumulate at fluid interfaces in the environment. Biologically, metal ion binding at cellular interfaces has been suggested to play a role in the misfolding of amyloidogenic proteins, one of the key events in neurodegenerative diseases such as Alzheimer's.<sup>44</sup> That certain metal ions can more strongly bind the carboxylate groups of surfactants such as fatty acids that make up cellular membranes has implications for metal ions accessibility to amyloid proteins at membranes that may affect their folding behavior.

## ■ ASSOCIATED CONTENT

### 📄 Supporting Information

Figures S1–S5 and Tables S1 and S2. This material is available free of charge via the Internet at <http://pubs.acs.org>.

## ■ AUTHOR INFORMATION

### Corresponding Author

\*E-mail [richmond@uoregon.edu](mailto:richmond@uoregon.edu); Fax 541-346-3422; Ph 541-346-0116.

### Notes

The authors declare no competing financial interest.

## ■ ACKNOWLEDGMENTS

The work has been supported by the National Science Foundation under Award CHE-1051215.

## ■ REFERENCES

- (1) Robertson, A. P.; Leckie, J. O. Acid/Base, Copper Binding, and  $\text{Cu}^{2+}/\text{H}^+$  Exchange Properties of a Soil Humic Acid, an Experimental and Modeling Study. *Environ. Sci. Technol.* **1999**, *33*, 786–795.
- (2) Ramos, M. A.; Fiol, S.; Lopez, R.; Antelo, J. M.; Arce, F. Analysis of the Effect of pH on  $\text{Cu}^{2+}$  - Fulvic Acid Complexation Using a Simple Electrostatic Model. *Environ. Sci. Technol.* **2002**, *36*, 3109–3113.
- (3) Kretzschmar, R.; Sticher, H. Transport of Humic-Coated Iron Oxide Colloids in a Sandy Soil: Influence of  $\text{Ca}^{2+}$  and Trace Metals. *Environ. Sci. Technol.* **1997**, *31*, 3497–3504.
- (4) Christl, I.; Kretzschmar, R. C-1s NEXAFS Spectroscopy Reveals Chemical Fractionation of Humic Acid by Cation-Induced Coagulation. *Environ. Sci. Technol.* **2007**, *41*, 1915–1920.
- (5) Teot, A. S.; Daniels, S. L. Flocculation of Negatively Charged Colloids by Inorganic Cations and Anionic Polyelectrolytes. *Environ. Sci. Technol.* **1969**, *3*, 825.
- (6) Rey-Castro, C.; Mongin, S.; Huidobro, C.; David, C.; Salvador, J.; Lluís Garces, J.; Galceran, J.; Mas, F.; Puy, J. Effective Affinity Distribution for the Binding of Metal Ions to a Generic Fulvic Acid in Natural Waters. *Environ. Sci. Technol.* **2009**, *43*, 7184–7191.
- (7) Porasso, R. D.; Benegas, J. C.; Van Den Hoop, M. G. T.; Paoletti, S. Analysis of Trace Metal Humic Acid Interactions Using Counterion Condensation Theory. *Environ. Sci. Technol.* **2002**, *36*, 3815–3821.
- (8) Rebhun, M.; Meir, S.; Laor, Y. Using Dissolved Humic Acid to Remove Hydrophobic Contaminants from Water by Complexation-Flocculation Process. *Environ. Sci. Technol.* **1998**, *32*, 981–986.
- (9) Saito, T.; Koopal, L. K.; Nagasaki, S.; Tanaka, S. Analysis of Copper Binding in the Ternary System  $\text{Cu}^{2+}$ /Humic Acid/Goethite at Neutral to Acidic Ph. *Environ. Sci. Technol.* **2005**, *39*, 4886–4893.
- (10) Voet, D.; Voet, J. G.; Pratt, C. W. *Fundamentals of Biochemistry: Life at the Molecular Level*; Wiley: New York, 2006.
- (11) Yazdaniyan, M.; Yu, H.; Zograf, G.; Kim, M. W. Divalent-Cation Stearic-Acid Monolayer Interactions at the Air-Water-Interface. *Langmuir* **1992**, *8*, 630–636.
- (12) Liu, M. H.; Kira, A.; Nakahara, H.; Fukuda, K. Complex Formation between Monolayers of Long-Chain Imidazole and Benzimidazole Derivatives and Transition Metal Ions. *Thin Solid Films* **1997**, *295*, 250–254.
- (13) Simon Kutscher, J.; Gericke, A.; Hühnerfuss, H. Effect of Bivalent Ba, Cu, Ni, and Zn Cations on the Structure of Octadecanoic Acid Monolayers at the Air-Water Interface as Determined by External Infrared Reflection-Absorption Spectroscopy. *Langmuir* **1996**, *12*, 1027–1034.
- (14) Gericke, A.; Hühnerfuss, H. The Effect of Cations on the Order of Saturated Fatty-Acid Monolayers at the Air-Water-Interface as Determined by Infrared Reflection-Absorption Spectrometry. *Thin Solid Films* **1994**, *245*, 74–82.
- (15) Du, X. Z.; Liang, Y. Q. Molecular Structure of Lead N-Octadecanoyl-l-Alaninate Langmuir-Blodgett Film. *J. Phys. Chem. B* **2001**, *105*, 6092–6096.
- (16) Ren, Y.; Iimura, K.; Kato, T. Structure of Barium Stearate Films at the Air/Water Interface Investigated by Polarization Modulation Infrared Spectroscopy and Pi-A Isotherms. *Langmuir* **2001**, *17*, 2688–2693.
- (17) Hühnerfuss, H.; Neumann, V.; Stine, K. J. Role of Hydrogen Bond and Metal Complex Formation for Chiral Discrimination in Amino Acid Monolayers Studied by Infrared Reflection - Absorption Spectroscopy. *Langmuir* **1996**, *12*, 2561–2569.
- (18) Tang, C. Y.; Allen, H. C. Ionic Binding of  $\text{Na}^+$  Versus  $\text{K}^+$  to the Carboxylic Acid Headgroup of Palmitic Acid Monolayers Studied by Vibrational Sum Frequency Generation Spectroscopy. *J. Phys. Chem. A* **2009**, *113*, 7383–7393.
- (19) Tang, C. Y.; Huang, Z.; Allen, H. C. Binding of  $\text{Mg}^{2+}$  and  $\text{Ca}^{2+}$  to Palmitic Acid and Deprotonation of the COOH Headgroup Studied by Vibrational Sum Frequency Generation Spectroscopy. *J. Phys. Chem. B* **2010**, *114*, 17068–17076.
- (20) Tang, C. Y.; Huang, Z.; Allen, H. C. Interfacial Water Structure and Effects of  $\text{Mg}^{2+}$  and  $\text{Ca}^{2+}$  Binding to the COOH Headgroup of a

Palmitic Acid Monolayer Studied by Sum Frequency Spectroscopy. *J. Phys. Chem. B* **2011**, *115*, 34–40.

(21) Beaman, D. K.; Robertson, E. J.; Richmond, G. L. From Head to Tail: Structure, Solvation, and Hydrogen Bonding of Carboxylate Surfactants at the Organic-Water Interface. *J. Phys. Chem. C* **2011**, *115*, 12508–12516.

(22) McFearin, C. L.; Richmond, G. L. The Role of Interfacial Molecular Structure in the Adsorption of Ions at the Liquid-Liquid Interface. *J. Phys. Chem. C* **2009**, *113*, 21162–21168.

(23) Bain, C. D.; Davies, P. B.; Ong, T. H.; Ward, R. N.; Brown, M. A. The Structure of Interfaces Probed by Sum-Frequency Spectroscopy. *Surf. Interface Anal.* **1991**, *17*, 529–530.

(24) Lim, M.; Hochstrasser, R. M. Unusual Vibrational Dynamics of the Acetic Acid Dimer. *J. Chem. Phys.* **2001**, *115*, 7629–7643.

(25) Goates, S. R.; Schofield, D. A.; Bain, C. D. A Study of Nonionic Surfactants at the Air–Water Interface by Sum-Frequency Spectroscopy and Ellipsometry. *Langmuir* **1999**, *15*, 1400–1409.

(26) Brown, M. G.; Raymond, E. A.; Allen, H. C.; Scatena, L. F.; Richmond, G. L. The Analysis of Interference Effects in the Sum Frequency Spectra of Water Interfaces. *J. Phys. Chem. A* **2000**, *104*, 10220–10226.

(27) Ota, S. T.; Richmond, G. L. Uptake of SO<sub>2</sub> to Aqueous Formaldehyde Surfaces. *J. Am. Chem. Soc.* **2012**, *134*, 9967–9977.

(28) Freitas, A. A.; Quina, F. H.; Carroll, F. A. Estimation of Water–Organic Interfacial Tensions. A Linear Free Energy Relationship Analysis of Interfacial Adhesion. *J. Phys. Chem. B* **1997**, *101*, 7488–7493.

(29) Apostoluk, W.; Drzymala, J. An Improved Estimation of Water–Organic Liquid Interfacial Tension Based on Linear Solvation Energy Relationship Approach. *J. Colloid Interface Sci.* **2003**, *262*, 483–488.

(30) Kendrick, M. J. *Metals in Biological Systems*; E. Horwood: Harlow, Essex, 1992.

(31) Weschler, C. J.; Mandich, M. L.; Graedel, T. E. Speciation, Photosensitivity, and Reactions of Transition-Metal Ions in Atmospheric Droplets. *J. Geophys. Res.: Atmos.* **1986**, *91*, 5189–5204.

(32) Colthrup, N. B.; Daly, L. H.; Wiberly, S. E. *Introduction to Infrared and Raman Spectroscopy*; Academic Press: New York, 1964.

(33) McFearin, C. L.; Beaman, D. K.; Moore, F. G.; Richmond, G. L. From Franklin to Today: Toward a Molecular Level Understanding of Bonding and Adsorption at the Oil-Water Interface. *J. Phys. Chem. C* **2009**, *113*, 1171–1188.

(34) Gragson, D. E.; Richmond, G. L. Probing the Structure of Water Molecules at an Oil/Water Interface in the Presence of a Charged Soluble Surfactant through Isotopic Dilution Studies. *J. Phys. Chem. B* **1998**, *102*, 569–576.

(35) Ji, N.; Ostroverkhov, V.; Tian, C. S.; Shen, Y. R., Characterization of Vibrational Resonances of Water-Vapor Interfaces by Phase-Sensitive Sum-Frequency Spectroscopy. *Phys. Rev. Lett.* **2008**, *100*.

(36) Tackett, J. E. Ft-Ir Characterization of Metal Acetates in Aqueous-Solution. *Appl. Spectrosc.* **1989**, *43*, 483–489.

(37) Du, X. Z.; Liang, Y. Q. Structure Control of Ion Exchange in N-Octadecanoyl-L-Alanine Langmuir-Blodgett Films Studied by FTIR Spectroscopy. *Langmuir* **2000**, *16*, 3422–3426.

(38) Lu, Y. Q.; Miller, J. D. Carboxyl Stretching Vibrations of Spontaneously Adsorbed and LB-Transferred Calcium Carboxylates as Determined by FTIR Internal Reflection Spectroscopy. *J. Colloid Interface Sci.* **2002**, *256*, 41–52.

(39) Alvarez-Puebla, R. A.; Valenzuela-Calahorra, C.; Garrido, J. J. Retention of Co(II), Ni(II), and Cu(II) on a Purified Brown Humic Acid. Modeling and Characterization of the Sorption Process. *Langmuir* **2004**, *20*, 3657–3664.

(40) Cotton, F. A. *Advanced Inorganic Chemistry*; Wiley: New York, 1999.

(41) Conboy, J. C.; Messmer, M. C.; Richmond, G. L. Investigation of Surfactant Conformation and Order at the Liquid-Liquid Interface by Total Internal Reflection Sum-Frequency Vibrational Spectroscopy. *J. Phys. Chem.* **1996**, *100*, 7617–7622.

(42) Conboy, J. C.; Messmer, M. C.; Richmond, G. L. Dependence of Alkyl Chain Conformation of Simple Ionic Surfactants on Head

Group Functionality as Studied by Vibrational Sum-Frequency Spectroscopy. *J. Phys. Chem. B* **1997**, *101*, 6724–6733.

(43) Walker, R. A.; Conboy, J. C.; Richmond, G. L. Molecular Structure and Ordering of Phospholipids at a Liquid-Liquid Interface. *Langmuir* **1997**, *13*, 3070–3073.

(44) Hoernke, M.; Koksche, B.; Brezesinski, G. Influence of the Hydrophobic Interface and Transition Metal Ions on the Conformation of Amyloidogenic Model Peptides. *Biophys. Chem.* **2010**, *150*, 64–72.